 

PACS numbers: 42.25.Ja; 78.20.Jg; 42.70.Mp; 42.79.Ci
DOI: 10.1070/QE2010v040n02ABEH014127

# Time-domain polarisation scrambler on one bulk $LiNbO_3$ crystal with quadrupole electrodes

B.L. Davydov, V.Yu. Mironov

***Abstract*. As distinct from the classic Billings depolariser, a simple time-domain polarisation scrambler can be made on one crystal possessing a threefold axis among its symmetry elements and displaying a linear electro-optical effect (Pockels effect). We demonstrate a polarisation scrambler on a $LiNbO_3$ uniaxial crystal with two pairs of electrodes to which two harmonic voltages identical in amplitude and differing in phase by 90° are applied. The residual degree of polarisation of the depolarised light, quantified by the polarisation extinction ratio, is less than 0.1 dB. Tolerances on the crystal orientation and the phase difference between the control voltages are estimated. The quality of the crystal is shown to be critical to the performance of the scrambler.**

***Keywords***: *polarisation scrambler, dual transverse Pockels effect, $LiNbO_3$.*

## 1. Introduction

Among components of optical measurement systems are laser light depolarisers, which average the polarisation states of light over time (Billings depolarisers [1]), wavelengths (Lyot depolarisers [2]) or multiple zones of the beam cross section (Cornu spatial depolarisers [3]). To depolarise laser beams with small cross sections and narrow bandwidths, use is typically made of the first type of depolariser, which in some cases improves the performance of optical devices. For example, the use of light unpolarised on a time average at the input of a fibre ring interferometer or in its loop ensures polarisation reciprocity of the interferometer with no polarisation filter and reduces the noise arising from polarisation fluctuations in isotropic single-mode optical fibres in response to changes in environment [4, 5]. The use of depolarisers in heterodyne (coherent) lidar systems enables elimination of the signal fading due to polarisation fluctuations of the backscattered radiation [6].

In this paper, we present the results of a study of a simple-design time-domain collimated laser beam polarisation scrambler on one lithium niobate ($LiNbO_3$) crystal.

**B.L. Davydov, V.Yu. Mironov** V.A. Kotel'nikov Institute of Radio Engineering and Electronics (Fryazino Branch), Russian Academy of Sciences, pl. Akademika Vvedenskogo 1, 141190 Fryazino, Moscow region, Russia; e-mail: bld_res2000@rambler.ru

Received 1 April 2009; revision received 1 December 2009
*Kvantovaya Elektronika* **40** (2) 183 – 187 (2010)
Translated by O.M. Tsarev

The classic bulk time-domain depolariser design proposed by Billings in 1951 includes at least two electro-optical crystals as independent, ac electric field controlled waveplates with an angle of 45° between their phase axes. After such a depolariser, the azimuthal angle of the beam polarisation ellipse varies in space, and its ellipticity changes many times. This corresponds to a uniform coverage of the entire Poincare sphere with polarisation states, with the polarisation point being in each state for the same length of time. This type of time-domain depolarisation can be considered ideal because it ensures all possible polarisation states. After such a depolariser, the power of the randomly polarised input light signal will always be equally distributed between signals with any orthogonal polarisation states. As a result, the accumulated time-averaged signal of a polarisation-sensitive receiver placed behind the depolariser becomes independent of the light polarisation at the depolariser input. However, because the device has a rather complex design and is difficult to control, ideal depolarisers are used rather rarely and are essentially missing in the market.

In practice, one typically uses 'linearly polarised' receivers, differing in their sensitivity to two orthogonal linear (plane) beam polarisations, rather than receivers with elliptical (or circular) eigenpolarisations. The power of a randomly polarised input signal is then equally distributed not between any orthogonal polarisation states but between orthogonal plane-polarised states (like in heterodyne lidars). A simpler depolarisation method can then be applied, involving rapid uniform rotation of the polarisation ellipse about the wave vector of the light, with no changes in ellipticity. Such rotation corresponds to circular motion of the polarisation point in a plane normal to the polar axis of the Poincare sphere [7]. This type of depolarisation can be considered pseudo-depolarisation. It should, however, be kept in mind that in real measurements it can only be used when there is no additional optically anisotropic component between the pseudo-depolariser and receiver. One example of such a component is isotropic, non-polarisation-maintaining optical fibre as a means of delivering an optical signal to a remote receiver.

Pseudo-depolarisation is easier to achieve than ideal, Billings depolarisation. For example, polarised light can be passed through a rapidly rotating half-wave ($\lambda/2$) plate at normal incidence. At the same time, using electro-optical crystals having a threefold rotation axis, one can design a substantially more convenient analogue of a rotating $\lambda/2$ plate, controlled electrically rather than mechanically.

## 2. Time-domain polarisation scrambler on a crystal displaying a dual transverse Pockels effect

The so-called dual transverse Pockels effect is displayed by crystals that have a threefold axis and exhibit a linear electro-optical effect [8, 9]. The effect occurs when light travels along the threefold axis and an electric field is applied to the crystal in an arbitrary direction normal to the axis. Among the most widespread electro-optical materials having this symmetry element ($SiO_2$, $LiNbO_3$, $LiTaO_3$, GaAs, CdTe, ZnSe and others), the one most frequently used in the visible and near-IR is $LiNbO_3$ (uniaxial crystals, symmetry class 3m), which is transparent in these spectral regions and exhibits the strongest electro-optical effect for the above light and field directions. As a result of the Pockels effect in this material [9], an initially circular cross section of the optical indicatrix in the (001) plane, normal to the optical axis (parallel to the threefold axis of $LiNbO_3$, [001], denoted as $Z$), becomes elliptical when an electric field $\boldsymbol{E}$ is applied in an arbitrary direction in the (001) plane. The axes of the ellipse make an angle $\alpha$ with the crystallographic axes $X$ and $Y$:

$$\tan 2\alpha = E_X/E_Y, \tag{1}$$

where $E_X$ and $E_Y$ are the projections of $\boldsymbol{E}$ onto the $X$ and $Y$ axes. Note that only in the configuration in question is the phase difference $\delta$ between the orthogonally polarised waves emerging from the crystal dependent only on the magnitude of the field, $|\boldsymbol{E}| = E = (E_X^2 + E_Y^2)^{1/2}$:

$$\delta = (2\pi/\lambda)n_o^3 r_{22} EL = (2\pi/\lambda)n_o^3 r_{22} VL/d, \tag{2}$$

where $\lambda$ is the incident wavelength; $n_o$ is the ordinary refractive index of the crystal; $r_{22}$ is the active component of the electro-optical tensor $r_{ik}$; $L$ is the electrode length along the light direction in the crystal; $V$ is the voltage applied to the electrodes; and $d$ is the electrode separation (crystal of square cross section).

It follows from (1) that, when $E_X$ and $E_Y$ harmonic fields with the same amplitude and the same circular frequency $\omega$, e.g. $E_X = E_0 \sin \omega t$ and $E_Y = E_0 \cos \omega t$, generated by two independent ac sources, are applied with a phase shift $\varphi = \pi/2$, we have $2\alpha = \omega t$ (equality of the two tangents). The situation is equivalent to using a fixed, nonrotating waveplate whose phase axis, however, steadily rotates about the wave vector of the light at a rate $d\alpha/dt = \omega/2$. It follows from (2) that, taking $E_0 = E_\pi$, where $E_\pi$ is the half-wave voltage for the given electro-optical configuration, we obtain a complete electro-optical analogue of a rotating $\lambda/2$ plate. The polarisation ellipse of light passing through such a $\lambda/2$ plate will steadily rotate about the wave vector of the light at a rate $\omega$. If the rotation period will be far shorter than the measurement time, any relatively slow varying polarisation states of the beam entering the crystal will be time-averaged.

## 3. Experimental and results

To experimentally verify the above, we used the setup shown schematically in Fig. 1. The light source (*1*) was a single-mode He–Ne laser ($\lambda = 632.8$ nm, $P_{out} = 0.5$ mW) or a power-stabilised unpolarised superluminescent emitter: a diode-pumped $Yb^{3+}$-doped isotropic silica fibre. The stable, unpolarised Gaussian beam from the latter source ($\lambda_{mid} = 1067$ nm, $\Delta\lambda = 20$ nm, $P_{out} = 12$ mW) was collimated by a gradient-index lens to a diameter of 0.5 mm and polarised by a Rochon prism (*2*) (certified polarisation extinction ratio of at least 50 dB). The aperture (*3*) was $\sim 1.0$ mm in diameter. It was used to select the most uniform zone of the crystalline polarisation scrambler (*4*). The scrambler had dimensions of 2.5, 2.5 and 34 mm along the $X$, $Y$ and $Z$ axes, respectively, and was fabricated from a congruent $LiNbO_3$ crystal* (Fig. 2). Electrodes were made on the lateral surfaces of the sample by evaporating gold on top of a chromium underlayer (electrode dimensions, $2.0 \times 33$ mm). To prevent surface interelectrode breakdown, the electrodes were potted in epoxy.

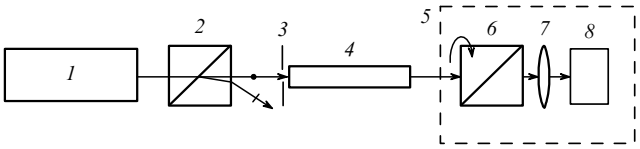


**Figure 1.** Experimental configuration: (*1*) He–Ne laser ($\lambda = 632.8$ nm) or superluminescent emitter: diode-pumped ($\lambda_{mid} = 1067$ nm, $\Delta\lambda = 20$ nm) $Yb^{3+}$-doped silica fibre; (*2*) polariser (Rochon prism); (*3*) 1-mm-diameter aperture; (*4*) $LiNbO_3$ crystal with quadrupole electrodes; (*5*) extinction meter; (*6*) analyser (Thompson prism); (*7*) lens focusing the beam onto the active area of the photodetector; (*8*) Anritsu ML9001A photodetector.

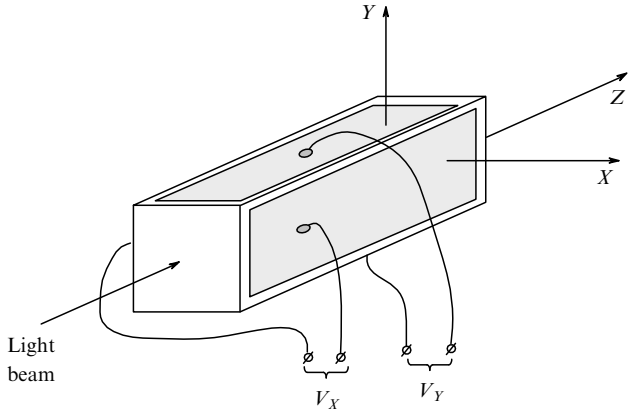


**Figure 2.** Geometry of the $LiNbO_3$ crystal and electrodes. $V_X$ and $V_Y$ are harmonic voltages.

Before epoxy potting, thin copper wires (voltage leads) were attached to the electrodes with a conductive cement.

The polarisation of the beam passed through the scrambler (Fig. 1) was analysed using an extinction meter (*5*) composed of a manually rotated Thompson prism (*6*), lens (*7*) and photodetector (*8*), which had an active area of $\sim 3$ mm diameter and a dynamic power measurement range from picowatts to 10 mW (over 60 dB). The residual degree of polarisation of the beam emerging from the scrambler was evaluated from the polarisation extinction ratio

*The half-wave voltages of the $LiNbO_3$ crystal were evaluated from the following values [10]: $r_{22}$ (1067 nm) $= 5.6 \times 10^{-12}$ m $V^{-1}$, $r_{22}$ (632.8 nm) $= 6.8 \times 10^{-12}$ m $V^{-1}$ (the $r_{22}$ values are given for the low frequencies used in our experiments), $n_o$ (1067nm) $= 2.2323$, $n_o$ (632.8 nm) $= 2.2866$, $L/d = 13.2$.

$$\varepsilon = 10\log(I_{max}/I_{min}), \quad (3)$$

where $I_{max}$ and $I$ are the maximum and minimum average intensities of the orthogonally polarised beam components at the photodetector (*8*).

The optical system was aligned by passing light beams along the optical axis $Z$ of the crystalline sample (*4*) so as to minimise the influence of optical inhomogeneities and stress-induced parasitic residual birefringence in the $LiNbO_3$ crystal on the initial plane-polarised states of the beams [at both wavelengths, the extinction ratios of the beams just in front of the scrambler (*4*) were at least 50 dB].

The $V_X$ and $V_Y$ harmonic control voltages were supplied from 50-Hz mains (time constant in the extinction measurements, $\sim 1$ s) through a variable transformer and an additional, isolation transformer, whose output winding was connected to a bridge circuit which ensured a phase shift from 0 to 180°, with two output voltages identical in amplitude [11]. The circuit and the corresponding vector diagram of active voltages are shown in Fig. 3. The phase shift $\varphi$ was varied using a dual potentiometer ($R_1 = R_2 = 51$ kΩ), which simultaneously varied the two resistances (either reducing or increasing both) at fixed capacitances $C_1 = C_2 = 0.1$ μF in the bridge. The phase $\varphi$ was determined as

$$\varphi = 180^\circ - 2\arctan(V_C/V_R), \quad (4)$$

where $V_C$ and $V_R$ are the voltages measured by a high-resistance digital voltmeter across either capacitance and either resistance.

For comparison with experiment, we calculated the polarisation extinction ratio as a function of harmonic control voltages differing in phase by 90° for 1067-nm light travelling along the optical axis of $LiNbO_3$. We used the classic formula for the intensity $I$ of light transmitted by an optical system comprising a source of monochromatic plane-polarised light, a crystalline plate ($LiNbO_3$ crystal) ensuring a relative phase shift $\delta$ given by (2) and an analyser [12]:

$$I = I_0[\cos^2(\beta - \alpha) - \sin(2\alpha)\sin(2\beta)\sin^2(\delta/2)], \quad (5)$$

where $I_0$ is the intensity incident on the crystalline plate; $\alpha$ is the angle between the plane of polarisation of the incident beam and one of the axes of the elliptical section of the indicatrix across the beam direction [formula (1)]; and $\beta$ is the angle between the direction of the output light's electric field oscillation and the same axis of the ellipse. (Since the polarisation analysis directions were orthogonal and, in our experiments, were fixed relative to the plane of polarisation of the incoming beam, $\beta$ was taken to be equal to $\alpha$ and $\alpha + 90^\circ$.)

In the calculations, we assumed that the input beam with $\lambda = 1067$ nm was completely plane-polarised and that the $LiNbO_3$ crystal was optically perfect and did not reduce the polarisation extinction ratio of light travelling along its optical axis. The intensities of the light with orthogonal polarisations at the analyser output were computed at 1-μs intervals and were then summed up and averaged over a time $t = 1$ s. Using the average intensities, the output extinction ratio was determined by Eqn (3) for each total control voltage value.

The measurement and calculation results are presented in Figs 4 and 5. In particular, Fig. 4 demonstrates good performance of the polarisation scrambler at both wavelengths. When the half-wave voltages and optimal crystal orientation are reached, the residual degree of polarisation is below 0.1 dB in both the IR [curve (*1*)] and red [curve (*3*)] spectral regions. The measured effective control half-wave voltages [$V_{eff}(1067\text{ nm}) \approx 550$ and 250 V] are about 20 % higher than the calculated values [$V_{eff}(1067\text{ nm}) \approx 460$ and

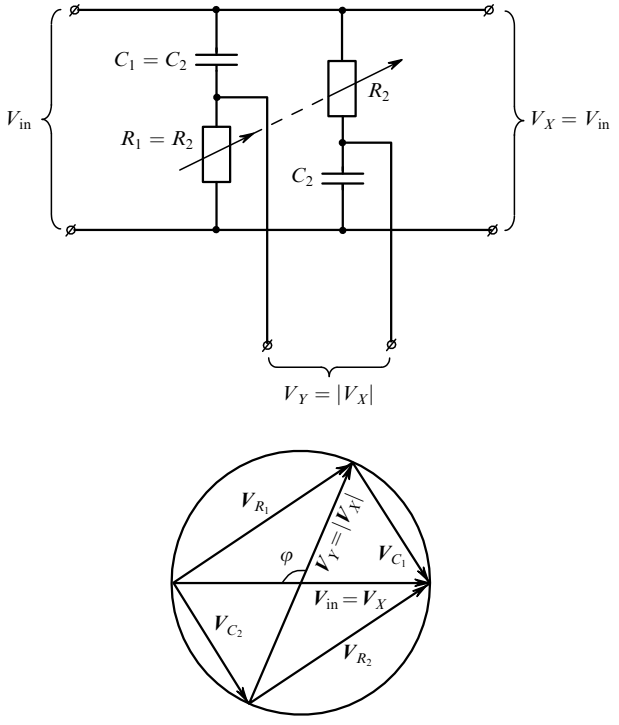


**Figure 3.** Phase-shift bridge supplying $V_X$ and $V_Y$ control voltages and the corresponding voltage vector diagram.

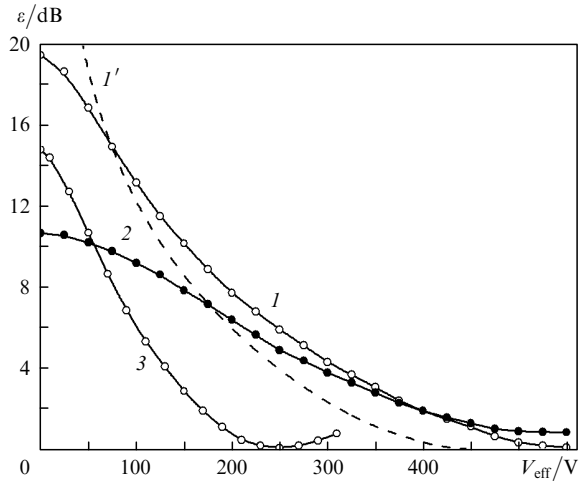


**Figure 4.** Polarisation extinction ratio of the output light as a function of effective control voltages differing in phase by 90°, $V_{eff\,X} = V_{eff\,Y} = V_{eff}$, for two wavelengths and two $LiNbO_3$ crystal orientations: (*1*) beam axis almost parallel to the optical axis of the crystal, $\lambda = 1067$ nm; (*1′*) calculation results corresponding to the experimental data (*1*); (*2*) beam axis 25′ off the optical axis of the crystal, $\lambda = 1067$ nm; (*3*) beam axis almost parallel to the optical axis of the crystal, $\lambda = 632.8$ nm.

210 V], which can be considered reasonable agreement given the moderate quality of our congruent $LiNbO_3$ crystal.

The deviation of curve (*1′*) from the experimental data is attributable to the imperfection of the crystal. In particular, at zero control voltages the parasitic stress in the crystal reduces the polarisation extinction ratio of the beam from 50 to $\sim$ 19 dB [see the initial, left portions of curves (*1*) and (*1′*)], and the distinction between the measured and calculated half-wave voltages is responsible for the discrepancy between their final, right-hand portions. Given these circumstances, the theoretical and experimental curves are qualitatively similar.

When the $LiNbO_3$ crystal is 25′ misoriented [curve (*2*)], the scrambler performance is, of course, lower, but not to an extent that it would be considered unsatisfactory: the residual degree of polarisation ($\sim$ 1 dB) is quite sufficient to solve many problems. Thus, we are led to conclude that the scrambler has sufficiently high performance and is not very sensitive to misorientation.

The performance of this crystalline sample and two others cut from the same large $LiNbO_3$ boule was found to be strongly influenced by local stress in the crystalline boule. In particular, one of the samples, cut from a zone with a fuzzy, distorted conoscopic image, proved unsuitable for polarisation scrambling: when control half-wave voltages were applied, the degree of polarisation decreased by just 3 dB relative to the initial one. This highlights that high-quality crystals must be selected for the fabrication of such polarisation scramblers. This can be done e.g. using a conoscopic cross: by monitoring its sharpness and distortion in various zones of a crystal with polished faces normal to its optical axis.

In Fig. 5, the polarisation extinction ratio calculated by Eqn (5) as a function of the missetting $\Delta\varphi$ of the phase difference $\varphi = 90^\circ$ between the $V_X$ and $V_Y$ control voltages is compared to experimental data obtained under the following conditions: superluminescent source ($\lambda_{mid}$ = 1067 nm), optimal crystal orientation (the crystal axis parallel to the beam axis) and control voltages equal to the half-wave voltage ($V_0 = V_\pi$). The calculations and experiments were performed for two schemes of polarisation scrambling analysis: (i) the average extinction ratio was measured and calculated for two orthogonal plane-polarised components with their planes of polarisation fixed at angles of 0 and 90° to those of the incoming beam; (ii) rotating the Thompson prism (*6*) of the extinction meter (*5*) (Fig. 1), we determined the largest extinction ratio, corresponding to the maximum degree of polarisation of the output beam, which occurred at analysis angles differing from 0 and 90° relative to the plane of polarisation of the incoming beam (in the calculations, the same variable angle was added to two $\beta$ angles differing by 90°). The former scheme, with a fixed analyser angle, is used most frequently; the latter is of interest because it demonstrates the rate of the increase in the degree of polarisation with increasing phase difference missetting $\Delta\varphi$. The increase is due to the fact that, at $\Delta\varphi \neq 0$, the crystal does not act as a half-wave plate, and its phase axis rotates unsteadily [see (1) and (2)]. As a result, the trajectory of the polarisation point on the Poincare sphere proves much more complex than a circle.

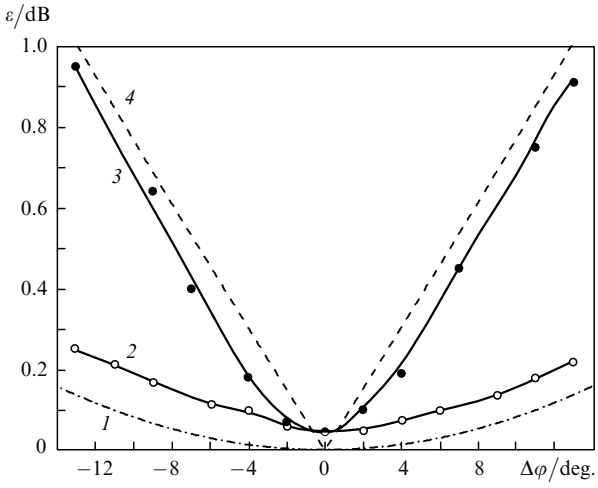


**Figure 5.** Polarisation extinction ratio of the light beam ($\lambda_{mid}$ = 1067 nm) against the missetting of the phase difference between the control half-wave voltages: (*1*) calculated data and (*2*) experimental results at fixed analyser angles (0 and 90°) relative to the plane of polarisation of the incoming beam; (*3*) measured maximum extinction ratio [with the polarisation analyser (Thompson prism) rotated] and (*4*) corresponding calculated curve.

The data in Fig. 5 can be used to determine the phase difference tolerance $\Delta\varphi$ at a phase setting $\varphi = 90^\circ$. In particular, even at arbitrary analyser angles and a rather large tolerance $\Delta\varphi = \pm 2^\circ$, the scrambler ensures a residual degree of polarisation of $\sim$ 0.1 dB (!). If the analyser is fixed, the phase difference tolerance is greater, especially at higher crystal quality [see curves (*1*) and (*2*), corresponding to ideal and imperfect crystals]. Moreover, our calculations show that, at $\Delta\varphi = \pm 90^\circ$, where the rotation angle of the phase axis is fixed at 22.5° and the phase delay $\delta$ varies according to a harmonic law, curve (*1*) tends to $\varepsilon \approx 3$ dB. This suggests that, even with such enormous phase errors, the device can be used as a coarse polarisation scrambler.

## 4. Conclusions

The present results demonstrate good performance of a simple time-domain polarisation scrambler made, as distinct from the classic Billings depolariser, on one $LiNbO_3$ crystal, displaying a dual transverse Pockels effect.

When two harmonic control voltages differ in phase by 90° and are equal to the half-wave voltage, the residual degree of polarisation of the light beam, quantified by the extinction ratio $\varepsilon = 10\log(I_{max}/I_{min})$, may be close to zero.

The performance of the scrambler is a relatively weak function of angular misorientation and phase difference missetting, which enables a simple design.

The quality of the crystalline boule has a strong effect on the performance of the polarisation scrambler fabricated from it.

Light propagation along the optical axis of the crystal ensures high thermal stability of the device owing to the lack of thermally induced birefringence. This implies that, at a constant applied half-wave voltage, the scrambler acts as a half-wave plate in a wide temperature range.

## References

1. Billings B.H. *J. Opt. Soc. Am.*, **41** (12), 996 (1951).
2. Mochizuki K. *Appl. Opt.*, **23** (19), 3284 (1984).
3. McGuire J.P., Chipman R.A. *Opt. Eng.*, **29** (12), 1478 (1990).

4. Alekseev E.I., Bazarov E.N., Izraelyan V.G., Kurbatov A.V. *Pis'ma Zh. Eksp. Teor. Fiz.*, **9** (14), 837 (1983).
5. Alekseev E.I., Bazarov E.N., Izraelyan V.G., Kovalenko V.G., *Kvantovaya Elektron.*, **12** (1), 174 (1985) [*Sov. J. Quantum Electron.*, **15** (1), 107 (1985)].
6. Protopopov V.V., Ustinov N.D. *Lazernoe geterodinirovanie* (Laser Heterodyning) (Moscow: Nauka, 1985) p. 5.
7. Shurcliff W.A. *Polarized Light: Production and Use* (Cambridge: Harvard Univ. Press, 1962; Moscow: Mir, 1965) pp 27, 126.
8. Buhrer C.F., Bloom L.K., Baird B.P. *Appl. Opt.*, **2** (8), 839 (1963).
9. Mustel' E.R., Parygin V.N. *Metody modulyatsii i skanirovaniya sveta* (Light Modulation and Scanning Methods) (Moscow: Nauka, 1970) p. 77.
10. http://www.inrad.com/pdf/inrad_datasheet_LNB.pdf.
11. Aseev B.P. *Fazovye sootnosheniya v radiotekhnike* (Phase Relations in Radio Engineering) (Moscow: Svyaz'izdat, 1954) pp. 49-59.
12. Sonin A.S., Vasilevskaya A.S. *Elektro-opticheskie kristally* (Electro-optical Crystals) (Moscow: Atomizdat, 1971) p. 41.